CONF-810415--3

LA-UR -81-101

TITLE: THE LINEAR-CHARACTERISTIC METHOD FOR SPATIALLY DISCRETIZING THE DISCRETE-ORDINATES EQUATIONS IN (X,Y)-GEOMETRY

AUTHOR(S): Edward W. Larsen and Raymond E. Alcouffe

SUBMITTED TO: ANS/ENS Joint Topical Meeting, Mathematical Methods in Nuclear Engineering, April 26-29, 1981, Munich, FRG

University of California

LOS ALAMOS SCIENTIFIC LABORATORY
Post Office Box 1663 Los Alamos, New Mexico 87545
An Affirmative Action/Equal Opportunity Employer

Form No. 836 R3
St. No. 2629
12/78

UNITED STATES
DEPARTMENT OF ENERGY
CONTRACT W-7405-ENG. 36

THE LINEAR CHARACTERISTIC METHOD FOR SPATIALLY DISCRETIZING THE DISCRETE ORDINATES EQUATIONS IN (X,Y)-GEOMETRY*

E. W. Larsen and R. E. Alcouffe
Theoretical Division
University of California
Los Alamos National Laboratory
Los Alamos, New Mexico 87545 USA

In this article a new linear characteristic (LC) spatial differencing scheme for the discrete ordinates equations in (x,y)-geometry is described and numerical comparisons are given with the diamond difference (DD) method. The LC method is more stable with mesh size and is generally much more accurate than the DD method on both fine and coarse meshes, for eigenvalue and deep penetration problems. The LC method is based on computations involving the exact solution of a cell problem which has spatially linear boundary conditions and interior source. The LC method is coupled to the diffusion synthetic acceleration (DSA) algorithm in that the linear variations of the source are determined in part by the results of the DSA calculation from the previous inner iteration. An inexpensive negative-flux fixup is used which has very little effect on the accuracy of the solution. The storage requirements for LC are essentially the same as that for DD, while the computational times for LC are generally less than twice the DD computational times for the same mesh. This increase in computational cost is offset if one computes LC solutions on somewhat coarser meshes than DD; the resulting LC solutions are still generally much more accurate than the DD solutions.

*This work was performed under the auspices of the U. S. Department of Energy.

THE LINEAR CHARACTERISTIC METHOD FOR SPATIALLY DISCRETIZING THE DISCRETE ORDINATES EQUATIONS IN (X,Y)-GEOMETRY

I. INTRODUCTION

The discrete-ordinates equations have been used for many years to approximate the neutron transport equation in large-scale numerical calculations. The traditional method of spatially discretizing these equations is the Diamond Difference (DD) method, although newer methods have been proposed [1-11], and one of these, the Linear Discontinuous (LD) method, has recently been implemented in several production codes [3,4].

A detailed study of spatial differencing schemes for the discrete-ordinates equations in various geometries has been undertaken at Los Alamos, and the results for slab geometry have been published [7]. These results indicate that for slab geometry, a new Linear Characteristic (LC) scheme outperforms the DD, LD, and other methods. In this article we describe our generalization of this method to (x,y)-geometry and present the results of some numerical comparisons with the DD method.

Roughly speaking, the philosophy of the LC method is to (i) represent the transport boundary conditions and source for a spatial cell by linear functions; (ii) solve the cell transport problem analytically by integrating along its characteristic lines; and (iii) generate, directly or indirectly from this analytic solution, linear representations to be used as boundary conditions for adjoining cells and to construct a scattering source for the next iteration. Step (iii) in this procedure is the most important one, since the manner in which it is implemented determines the speed and accuracy of the method, as well as its interaction with acceleration methods and the overall storage requirements of the code.

In slab geometry, "characteristic" methods following the above basic procedure have been developed by several authors [6,7,9]. Similar methods have also been developed by other authors for other geometries, although generally they are based on computing cell-vertex fluxes rather than cell-average and edge-average fluxes, as is done here. Lathrop's (x,y)-geometry Step Characteristic (SC) method [12] does utilize cell-average and edge-average fluxes, although his method employs constant (rather than linear) representations for the source and boundary conditions for each cell. Our (x,y)-geometry method can thus be regarded as a higher-order version of the SC method.

The LC method has evolved from its original conception over the course of numerical testing. In Sec. II we describe the development of this method, and in Sec. III we present the results of some numerical studies comparing the LC and DD methods. We conclude with a brief discussion in Sec. IV.

II. THEORY

To describe the LC method in (x,y)-geometry, let us consider a typical within-group transport problem for one spatial cell:

$$\mu \frac{\partial \psi}{\partial x} + \eta \frac{\partial \psi}{\partial y} + \sigma\psi = S_{av} + (x - \frac{h}{2}) S_x + (y - \frac{k}{2}) S_y ,$$

$$0 < x < h, \quad 0 < y < k, \quad \mu > 0, \quad \eta > 0 , \tag{2.1}$$

$$\psi(0,y) = \psi_L + (y - \frac{k}{2}) \theta_L \quad , \quad 0 < y < k \quad , \tag{2.2}$$

$$\psi(x,0) = \psi_B + (x - \frac{h}{2}) \theta_B \quad , \quad 0 < x < h \quad . \tag{2.3}$$

In an inner iteration, the source for each cell (right side of Eq. (2.1)) is prescribed and one sweeps from cell to cell through the system to obtain improved values of ψ; these are then used to update the source for the next iteration. Thus we shall discuss separately the problem of sweeping through the system with a prescribed source, and the problem of updating the source with the new values of ψ.

First we consider the sweeping part of the problem. In order to generate linear boundary data for adjoining cells, one must obtain linear representations of the angular flux exiting each cell. Thus, in the context of the cell problem (2.1) - (2.3), we require linear representations of the form

$$\psi(h,y) \approx \psi_R + (y - \frac{k}{2}) \theta_R \quad , \quad 0 < y < k \quad , \tag{2.4}$$

$$\psi(x,k) \approx \psi_T + (x - \frac{h}{2}) \theta_T \quad , \quad 0 < x < h \quad . \tag{2.5}$$

In the orignal LC method, these representations were determined by the following two-step procedure: (i) construct the analytic solution $\psi(x,y)$ of the cell problem (2.1) - (2.3); (ii) choose the representations (2.4) and (2.5) to exactly preserve the zero'th and first moments of ψ on the right and top edges of the cell. (This procedure owes a debt not only to Lathrop [12], but also to Vaidyanathan [6], who has emphasized the importance of preserving spatial moments of the analytic solution of cell problems.)

Step (i) is carried out by integrating the transport equation along its characteristic lines. The result can be written

$$\psi(x,y) = \Psi(x,y) + P_{av} + (x - \frac{h}{2}) P_x + (y - \frac{k}{2}) P_y \tag{2.6}$$

where

$$\Psi(x,y) = \begin{cases} [\alpha_L + (y - \frac{k}{2} - \frac{\eta}{\mu} x)\,\beta_L]\, e^{-\sigma x/\mu} & , \quad \mu y > \eta x \ , \\ [\alpha_B + (x - \frac{h}{2} - \frac{\mu}{\eta} y)\,\beta_B]\, e^{-\sigma y/\eta} & , \quad \mu y < \eta x \ , \end{cases} \tag{2.7}$$

and

$$P_x = \frac{S_x}{\sigma} \quad , \quad P_y = \frac{S_y}{\sigma} \quad , \tag{2.8}$$

$$P_{av} = \frac{S_{av}}{\sigma} - \frac{2}{\sigma}\left(\frac{\mu P_x}{h} + \frac{\eta P_y}{k}\right) \quad , \tag{2.9}$$

$$\alpha_L = \psi_L - P_{av} + \frac{h}{2} P_x \quad , \quad \beta_L = \theta_L - P_y \quad , \tag{2.10}$$

$$\alpha_B = \psi_B - P_{av} + \frac{k}{2} P_y \quad , \quad \beta_B = \theta_B - P_x \quad . \tag{2.11}$$

Step (ii) can now be carried out using this analytic form of ψ. All of the integrations can be performed explicitly, since the integrands involve at most the product of a second-order polynomial and an exponential.

The most efficient coding of the method for $\sigma \neq 0$ involves first computing the constants in Eqs. (2.8) - (2.11) and then manipulating and evaluating Eq. (2.7). However, this procedure is invalid for $\sigma = 0$ since all of the constants in Eqs. (2.8) - (2.11) become infinite as $\sigma \to 0$. (Mathematically, this occurs because of a removable singularity at $\sigma = 0$. The angular flux ψ actually depends continuously on σ as $\sigma \to 0$.) We handle this problem by utilizing a separate block of coding which treats specifically cell problems for which $\sigma = 0$. Also, we treat cells for which $0 < \sigma << 1$ in a third separate block of coding, since roundoff errors would otherwise become infinite as $\sigma \to 0$. Here we expand ψ in powers of σ, keeping terms only up to σ^5; this block of coding is used whenever

$$0 < \min\left(\frac{\sigma h}{|\mu|} \ , \ \frac{\sigma k}{|\eta|}\right) < .01 \quad .$$

The above method is not inherently positive, for the following reason. If the source and boundary conditions for the cell problem (2.1) - (2.3) are nonnegative, then ψ is nonnegative, and so ψ_R and ψ_T will be nonnegative. However, the values of θ_R and θ_T can be such that one or both of the representations (2.4), (2.5) become negative at certain points. We

have observed that these negativities can lead to negative cell-average angular and scalar fluxes. To prevent this, we alter the values of θ_R or θ_T by the minimum amount so that the new representations are nonnegative along the appropriate cell edges. For example, if $k\,|\theta_R| > 2\,\psi_R$, then we replace θ_R by $\xi\theta_R$, where $\xi = 2\psi_R/k|\theta_R|$. These adjustments guarantee that the linear representations (2.4) - (2.5) will be nonnegative as the system is swept cell by cell, provided of course that the sources and system boundary conditions are nonnegative.

The above method was tested on a variety of problems and was found to give good results compared to DD. (Cell-average fluxes for the above LC method were computed in each cell calculation using the balance equation, and these were compared to the DD cell-average fluxes. Integral quantities such as total absorptions and leakages were also computed.) However, the new method was found to be considerably more expensive per cell calculation than the DD method.

In an effort to reduce the calculational cost of the new method, we examined a number of schemes in which the first spatial moments of ψ are approximated in Eqs. (2.4) - (2.5) rather than computed exactly. This led to the following modification of the LC method.

Consider again the cell problem (2.1) - (2.3) and suppose for definiteness that

$$\rho = \frac{\mu k}{\eta h} < 1 \quad . \tag{2.12}$$

Then the characteristic line which emanates from the lower left corner of the spatial cell intersects the top edge of the cell at the point $x = \rho h$, $y = k$. We define ψ_R and θ_R as

$$\psi_R = \frac{1}{k}\int_0^k \psi(h,y')\,dy' \quad , \tag{2.13}$$

$$\theta_R = \frac{1}{k}\,[\psi(h,k) - \psi(h,0)] \quad . \tag{2.14}$$

To define θ_T, we note that the boundary conditions on the left edge of the cell influence $\psi(x,k)$ for $0 < x < \rho h$, while the boundary conditions on the bottom edge of the cell influence $\psi(x,k)$ for $\rho h < x < h$. Therefore, we compute separate linear representations of $\psi(x,k)$, analogous to the one above for $\psi(h,y)$, but for the two intervals $0 < x < \rho h$ and $\rho h < x < h$; then we choose the primary linear representation of $\psi(x,k)$, given by Eq. (2.5), to exactly preserve the zero-th and first spatial moments of this piecewise linear representation. The result is:

$$\psi_T = \rho\psi_{TL} + (1 - \rho)\,\psi_{TR} = \frac{1}{h}\int_0^h \psi(x',k)\,dx' \quad , \tag{2.15}$$

$$\theta_T = \frac{1}{\rho h}\,[\psi(\rho h - 0,k) - \psi(0,k)]\,\rho^3$$

$$+ \frac{1}{(1-\rho)h}\,[\psi(h,k) - \psi(\rho h + 0,k)]\,(1-\rho)^3$$

$$+ \frac{1}{h/2}\,[\psi_{TR} - \psi_{TL}]\,3\rho\,(1-\rho)\quad , \tag{2.16}$$

where

$$\psi_{TL} = \frac{1}{\rho h}\int_0^{\rho h} \psi(x',k)\,dx' \quad ,$$

$$\psi_{TR} = \frac{1}{(1-\rho)h}\int_{\rho h}^{h} \psi(x',k)\,dx' \quad .$$

Then ψ_R and ψ_T - given by Eqs. (2.13) and (2.15) - are the exact zero'th moments of ψ on the right and top edges of the cell, while θ_R and θ_T - given by Eqs. (2.14) and (2.16) - are suitable approximations to the first moments of ψ. (These approximations result in about a 20% savings in computational effort with very little loss of accuracy.) The linear representations (2.4) - (2.5), together with the formulas (2.13) - (2.16), the treatments for $\sigma = 0$ and $0 < \sigma << 1$, and the fixup described above, describe the sweeping part of an inner iteration in the LC method.

The second part of an inner iteration consists of updating the source. This was originally done in the LC method by constructing, for each cell and discrete-ordinate direction, the linear representation (given below in the context of the cell of Eq. (2.1))

$$\psi(x,y) \approx \psi_{av} + (x - \tfrac{h}{2})\,\psi_x + (y - \tfrac{k}{2})\,\psi_y \quad , \qquad 0 < x < h,\ 0 < y < k \quad , \tag{2.17}$$

where ψ_{av}, ψ_x, and ψ_y are determined from the zero'th and first-order balance equations, using ψ_L, θ_L, etc., as the zero'th and first-order moments of ψ on the cell edges. (In addition, ψ_x and ψ_y are multiplied by a suitable factor $0 < \xi < 1$ if the representation (2.17) becomes negative, so that the resulting representation is nonnegative in the cell.) These representations are folded into arrays which, upon the completion of the inner iteration, give the zero'th and first (or, approximations of the first) spatial moments within each cell of those angular moments of ψ which are needed for the scattering law. This procedure is straightforward and completely analogous to the way the boundary fluxes are treated, and it gives good results for problems with scattering. More-

over, it interacts well with rebalance [13]. However, it requires the storage of three times the number of source arrays as in the DD method, and for reasons which we do not fully understand, it interacts poorly with diffusion-synthetic acceleration (DSA).

To contend with these two serious difficulties, we completely altered the above strategy of updating the source for the next inner iteration and after some experimentation, settled on the following procedure, which is intimately connected with DSA. In a cell calculation, we now compute ψ at the outgoing vertex and, using the balance equation, ψ_{av}, but we do not compute ψ_x or ψ_y. The vertex fluxes are folded into an array which, at the end of the transport sweep, gives the scalar vertex fluxes, while the cell-average fluxes are treated just as in the DD method: they are folded into arrays which, at the end of the transport sweep, give those cell-average angular flux moments which are needed for the scattering law.

Thus, at the end of the transport sweep, cell-averaged angular flux moments and vertex scalar fluxes are available. (This is precisely the information which is required of the DD method by DSA.) Now a diffusion problem is solved in which the above information from the transport sweep appears as inhomogeneous terms [14]. The result of this diffusion calculation are vertex scalar fluxes, which we denote for the cell in Eq. (2.1) as $\hat{\phi}_{BL}$, $\hat{\phi}_{BR}$, $\hat{\phi}_{TL}$, and $\hat{\phi}_{TR}$. (The transport vertex scalar fluxes are denoted without hats.) Also, let S^*_{av} denote the cell-average source for this cell as computed using the values of ψ_{av} which were obtained from the transport sweep. (S^*_{av} is a function of angle if scattering is anisotropic.) Then the linear source which we use for the next inner iteration is

$$S(x,y) = S^*_{av} \left[\alpha + \left(x - \frac{h}{2}\right) \beta + \left(y - \frac{k}{2}\right) \gamma\right] \tag{2.18}$$

where

$$\alpha = \frac{\hat{\phi}_{TR} + \hat{\phi}_{BR} + \hat{\phi}_{TL} + \hat{\phi}_{BL}}{\phi_{TR} + \phi_{BR} + \phi_{TL} + \phi_{BL}} ,$$

$$\beta = \frac{2}{h} \frac{\hat{\phi}_{TR} + \hat{\phi}_{BR} - \hat{\phi}_{TL} - \hat{\phi}_{BL}}{\phi_{TR} + \phi_{BR} + \phi_{TL} + \phi_{BL}} ,$$

$$\gamma = \frac{2}{k} \frac{\hat{\phi}_{TR} - \hat{\phi}_{BR} + \hat{\phi}_{TL} - \hat{\phi}_{BL}}{\phi_{TR} + \phi_{BR} + \phi_{TL} + \phi_{BL}} .$$

In addition, we multiply β and γ by a suitable factor $0 < \xi < 1$ if the bracketed term in Eq. (2.18) becomes negative, so that the resulting term is nonnegative in the cell. Then the source S for the next inner iteration will be positive unless the scattering cross-sections are negative due to to an improper spherical harmonics truncation.

The above LC method generally interacts with DSA at least as well as the DD method, and moreover, the storage requirements for the source reduce to these for DD plus one array for the vertex scalar fluxes. (Essentially, the number of required source arrays has been reduced by one-third.) In addition, there is about a 15% savings in computional effort since ψ_x and ψ_y no longer have to be computed.

On the negative side, there is a minor loss of accuracy, but this is substantially outweighed by the advantages listed above.

III. NUMERICAL RESULTS

Here we present some numerical results from two three-group, isotropic scattering problems, the first a k-eigenvalue problem and the second a shielding problem. Due to their size and the characteristics of their cross sections, both problems are somewhat difficult for the DD method.

III.A. Eigenvalue Test Problem

The system is shown in Figure 1. Dimensions are given in centimeters. Regions I, II, and III are a fission, absorbing, and a scattering-shielding region respectively, and the cross sections are given (with dimension cm^{-1}) in Table 1.

A series of five calculations were performed using the DD and the LC methods. In each calculation the S_4 angular quadrature approximation was used and the number of (uniform) spatial cells in each region was varied as shown in Table 2. (The fine mesh is indicated in parentheses in Fig. 1.)

In Table 3 we present the eigenvalues for each case as computed with a convergence criterion of 10^{-6}. We also give the total number N of iterations and computation time T (in seconds) taken to converge the solution to a (greater) 10^{-4} error. (We do this because 10^{-4} is a more typical convergence criterion for eigenvalue problems.)

The fine mesh (Case 1) was chosen so that in the fission region a spatial cell is less than 0.1 mfp across; for this mesh one can hope that the solutions are nearly spatially converged. This is seen to be true for the LC eigenvalue, but not for the DD eigenvalue. Also, the interaction of the LC method with DSA is seen to be at least as good as that with DD. In interpreting the calculation times, we caution that neither the LC nor DD methods are fully optimized as to computational efficiency. For example, the DD code is TWOTRAN-DA, which has the algorithm for either an (x,y) or an (r,z) solution; this is less efficient than a straight (x,y) algorithm.

III.B Shielding Test Problem

The system is shown in Figure 2 and the cross sections for regions I and II are given in Table 4. A spatially flat source in the inner shaded region, with the normalized spectrum 0.739, 0.261, and 0.0 for groups 1, 2, and 3 respectively, drives the system.

This problem was solved numerically on a coarse and a fine spatial mesh (the number of cells for each mesh is indicated in parentheses in Figure 2), with an S_8 quadrature set, and with both the DD and LC methods. The convergence criterion was 10^{-4}, and in certain cases the solutions did not fully converge. The net groupwise leakages through the top and right edges of the system (L_T and L_R) for each method and spatial mesh are shown in Table 5. The LC results are observed to be quite stable with coarsening of the mesh, whereas the DD results are less so, particularly in the horizontal direction where the spatial cells are large as measured in mean free paths.

The number of iterations, the error if not fully converged (in parentheses) and the computation times are given in Table 6.

It is puzzling that the DD solution is fully converged on the coarse mesh but not on the fine mesh. However, this erratic behavior of the DD solution for large meshes is well-known and is one of the motivations for seeking a more stable and accurate differencing scheme.

We add that the above coarse mesh is about as coarse as it can be for both methods to converge. For instance, if the number of intervals in the outer region is reduced from 15 to 13, the DD method fails to converge and if it is reduced from 15 to 10, then both methods fail to converge.

Finally, we compared the cell-average scalar fluxes for the two methods in the cells along the right edge of the system. (See Figures 3 and 4.) The LC fluxes decrease monotonically from cell to cell in the upward direction while the DD fluxes display an overall decrease, but coupled with an oscillatory behavior. This, together with similar observations from other problems, indicates that the LC pointwise fluxes are more stable and accurate than the DD pointwise fluxes.

IV. DISCUSSION

In this article we have described the development of the LC method in (x,y)-geometry and have also given some numerical comparisons with the DD method. The LC method (coupled with the DSA algorithm as described in Sec. II) shows considerable promise of giving accurate and stable results on spatial meshes which are coarser than those appropriate for DD, especially for problems which are difficult for DD. The LC storage requirements are virtually the same as DD, and the LC computation times are often about equal to and rarely greater than twice the DD computation times, for the same mesh, and for problems in which both methods converge.

Nevertheless, the results given in this article should be viewed as work-in-progress rather than as definitive. The final form of the LC method is not settled for the following two reasons.

First, the interaction between LC and DSA is not properly understood and not fully ironed out. We expected DSA to interact better with LC than with DD, but we have found problems in which the interaction with LC is erratic (and, in fact, worse than with DD). Also, there are more difficult problems (characterized by very large cell sizes) in which neither LC nor DD (with DSA) converges. (However, as the cell sizes increase, DD is normally the first of the two methods to fail to converge.) To contend with these difficulties, it may be necessary to introduce modifications in both the LC and DSA algorithms.

Second, the LC method has not been tested on anisotropic scattering problems, and it may be necessary to introduce further changes in the method to achieve high accuracy. This possibility arises because the linear variation of the source in a cell is presently determined solely by the vertex scalar fluxes.

It is likely that the LC method, as strictly envisioned in this article, cannot be practically applied in curvilinear geometries. This is because the analytic solutions of cell problems consist of functions which are more complicated than a polynomial times an exponential, and which cannot be explicitly itegrated. Thus, unlike the situation in (x,y)-geometry, analytic expressions for the cell-edge and cell-average fluxes are not available. High-accuracy numerical integrals of course are available, but the extra computational cost would probably render the method uncompetative. The LC method of this article can however be easily extended to triangular mesh (x,y)-geometry problems. It can also be extended to (x,y,z)-geometry, although here algebraic difficulties occur which make the method appear somewhat less attractive.

In summary, the LC method in (x,y)-geometry requires more work to attain an optimal form. The main difficulty appears to lie in the interaction between the LC and the DSA algorithms. The goal, which we hope can be achieved, is a method which gives accurate and stable results for general types of problems and for relatively coarse spatial meshes.

REFERENCES

1. K. Takeuchi, J. Nucl. Sci. Tech., 8, 141 (1971).

2. J. R. Askew, "A Characteristics Formulation of the Neutron Transport Equation in Complicated Geometries," AEEW-M 1108, AEE Winfrith (1972).

3. T. R. Hill, "ONETRAN: A Discrete Ordinates Finite Element Code for the Solution of the One-Dimensional Multigroup Transport Equation," LA-5990-MS, Los Alamos Scientific Laboratory (1975).

4. T. J. Seed, W. F. Miller, Jr., and F. W. Brinkley, Jr., "TRIDENT: A Two-Dimensional, Multigroup, Triangular Mesh Discrete Ordinates, Explicit Neutron Transport Code," LA-6735-M, Los Alamos Scientific Laboratory (1977).

5. P. Barbucci and F. DiPasquantonio, Proc. of the Fifth International Conference on Reactor Shielding, Knoxville, Tennessee, April 17-23, 1977, Science Press, 711 (1977).

6. R. Vaidyanathan, Nucl. Sci. Eng., 71, 46 (1979).

7. R. E. Alcouffe, E. W. Larsen, W. F. Miller, Jr., and B. R. Wienke, Nucl. Sci. Eng., 71, 111 (1979).

8. E. W. Larsen, Trans. Am. Nucl. Soc., 33, 317 (1979).

9. D. V. Gopinath, A. Natarajan, and V. Sundararaman, Nucl. Sci. Eng., 75, 181 (1980).

10. R. D. Lawrence and J. J. Dorning, "A Discrete Nodal Integral Transport Theory Method for Multidimensional Reactor Physics and Shielding Calculations," Proc. of the 1980 ANS Topical Meeting on Advances in Reactor Physics and Shielding, Sun Valley, Idaho, Sept. 14 17, 1980.

11. W. F. Walters and R. D. O'Dell, "Nodal Methods for Discrete-Ordinates Transport Problems in (X,Y) Geometry," these proceedings.

12. K. D. Lathrop, J. Comp. Phys., 4, 475 (1969).

13. W. F. Walters, private communication.

14. R. E. Alcouffe, Nucl. Sci. Eng., 64, 344 (1977).

Table 1. Cross Sections for the Eigenvalue Test Problem

Region	Group (g)	χ	$\nu\sigma_f$	σ_T	$\sigma_{g\to g}$	$\sigma_{g-1\to g}$	$\sigma_{g-2\to g}$
I	1	0.7	0.0524	0.1440	0.0871	0	0
I	2	0.2	0.01	0.2591	0.2486	0.0453	0
I	3	0.1	0.006	0.4062	0.3883	0.0387	0.0001
II	1	0	0	0.1	0	0	0
II	2	0	0	0.3	0	0	0
II	3	0	0	5.0	0	0	0
III	1	0	0	0.2163	0.1760	0	0
III	2	0	0	0.3255	0.3236	0.0399	0
III	3	0	0	1.1228	0.9328	0	0

Table 2. Spatial Meshes for the Eigenvalue Test Problem

Case	Region I	Region II	Region III
1	24	8	24
2	12	4	12
3	6	2	6
4	3	1	3
5	1	1	1

Table 3. Results for the Eigenvalue Test Problem

Case	LC			DD		
	k_{eff}	N	T	k_{eff}	N	T
1	0.603616	18	50.20	0.603496	19	30.03
2	0.603606	20	9.26	0.603129	129	16.70
3	0.603526	24	2.93	0.601650	25	2.33
4	0.603102	30	1.34	0.595217	37	1.60
5	0.583862	44	1.24	0.550890	33	1.56

Table 4. Cross Sections for the Shielding Test Problem

Region	Group (g)	σ_T	$\sigma_{g\to g}$	$\sigma_{g-1\to g}$	$\sigma_{g-2\to g}$
I	1	0.2656	0.16	0	0
I	2	1.1745	1.101	0.1052	0
I	3	3.2749	3.2565	0.073	0
II	1	0.2163	0.176	0	0
II	2	0.3255	0.3236	0.0399	0
II	3	1.1228	0.9328	0.9828	0

Table 5. Leakages for the Shielding Test Problem

	L_R				L_T			
	Coarse		Fine		Coarse		Fine	
Group	LC	DD	LC	DD	LC	DD	LC	DD
1	8.74E-8	5.73E-8	8.88E-8	8.30E-8	9.86E-5	9.22E-5	9.89E-5	9.76E-5
2	4.69E-8	3.66E-8	4.85E-8	4.78E-8	6.19E-5	5.70E-5	6.22E-5	6.10E-5
3	9.90E-8	1.16E-7	1.00E-7	9.66E-8	1.42E-4	1.31E-4	1.43E-4	1.40E-4
Total	2.33E-7	2.10E-7	2.38E-7	2.27E-7	3.02E-4	2.81E-4	3.04E-4	2.99E-4

Table 6. Number of Iterations, Errors, and Computation Times for the Shielding Test Problem

	Coarse		Fine	
Group	LC	DD	LC	DD
1	9	30	20	37
2	33	69	14	74 (3E-3)
3	74 (3E-4)	55	33	74 (2E-3)
Total	116	154	67	185
Time (sec)	124.7	67.7	325.0	341.6

Figure 1. System for the Eigenvalue Test Problem

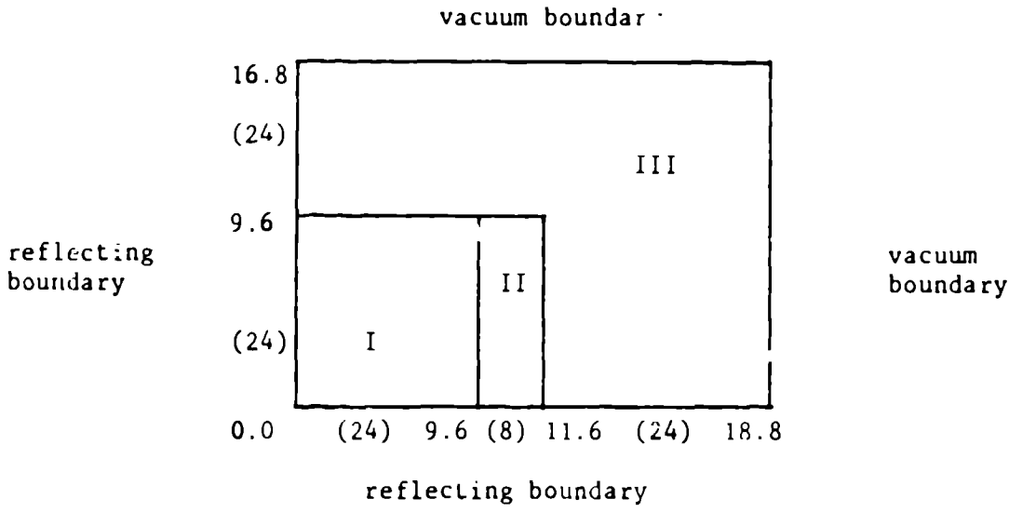

Figure 2. System for the Shielding Test Problem

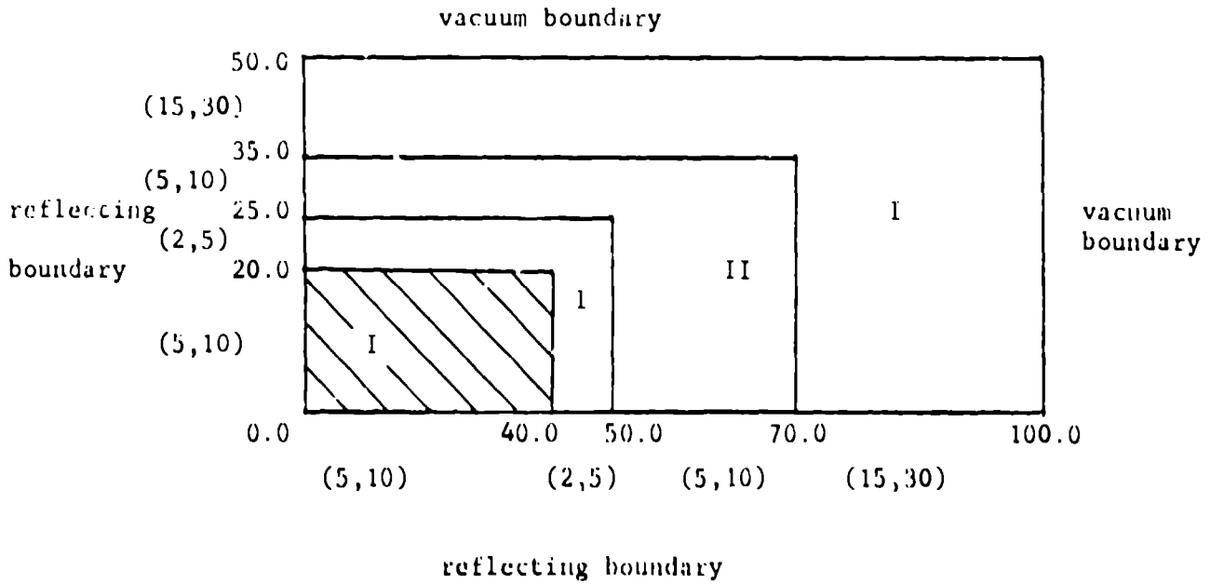

Figure 3. LC (——) and DD (x x x) Cell-Average Fluxes on Right Edge of Shielding Problem (Coarse Mesh).

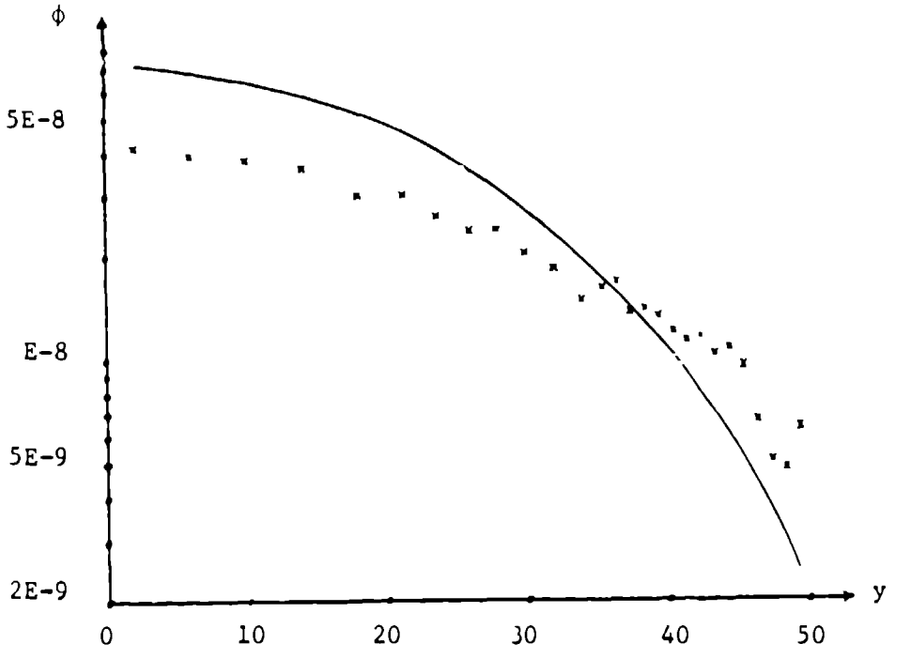

Figure 4. LC (——) and DD (x x x) Cell-Average Fluxes on Right Edge of Shielding Problem (Fine Mesh).